Analysis of End Effects in SAW IDTs Using the Finite Difference Method

Deepak Jatkar and Benjamin Beker
Department of Electrical and Computer Engineering
University of South Carolina
Columbia, South Carolina 29208

Abstract-**For high-performance SAW filter design the variation of charge distribution along the IDT fingers needs to be evaluated accurately. In this work, the finite difference method was used to study the effects of transverse (along the length of the fingers) and longitudinal (along the propagation direction) variation in charge distribution on the acoustic admittance of the IDT. A comparison was made between a full three-dimensional analysis of SAW IDTs, which includes the effects of bus bars, and the 2-D approximation to the same IDT.**

INTRODUCTION

Surface acoustic wave filters and resonators are gaining popularity in microwave circuits used in oscillators, mobile communication and digital systems. Attractive features of such devices are low insertion loss and tight frequency control. The physical basis for operation of the SAW is the electrostatic charge on its transducer acting as a source of the generated acoustic wave.

The frequency response of the SAW filter can be obtained from the Fourier transform of this charge distribution [1]. Therefore, the first step in the analysis of SAW IDTs involves the calculation of the charge distribution on its fingers. Various techniques have been used to obtain this charge distribution in the past. The most commonly used technique involves obtaining the charge distribution as a superposition of basic charge distribution functions [2]. The transducer response can then be obtained as a product of an "element factor" and an "array factor" [3-4]. However, this method ignores the end effects in both longitudinal and transverse directions. Some initial analysis of the transverse end effects has been carried out in [5]. More recently, the Green's function method was used to obtain the two-dimensional charge distribution on the fingers of the IDT and package [6-7]. However, the effects of the transverse variation in charge on acoustic admittance were not evaluated in that study.

In this work, the finite difference method was employed to study the transverse variation of the charge on a SAW IDT. The two-dimensional surface charge density (computed from the three-dimensional potential distribution) was used to obtain the acoustic admittance of the IDT. The results were compared to the two-dimensional approximation for different aperture lengths.

THEORY

The first step in calculating the frequency response of a SAW transducer is to obtain the charge distribution on the IDT fingers. Consider the SAW transducer shown in Fig. 1. For the frequency of operation and corresponding structure dimensions, the problem involves solving the Laplace equation in the two regions (1 and 2). Since most of piezoelectric substrates (region 2) are anisotropic, the equation to be solved (in three-dimensions) is given by

$$\nabla \cdot \left(\varepsilon_0 [\varepsilon(x,y,z)] \cdot \nabla\phi\right) = 0 \quad , \tag{1}$$

where [ε] stands for the permittivity tensor whose form is

$$[\varepsilon] = \begin{bmatrix} \varepsilon_{xx} & \varepsilon_{xy} & \varepsilon_{xz} \\ \varepsilon_{yx} & \varepsilon_{yy} & \varepsilon_{yz} \\ \varepsilon_{zx} & \varepsilon_{zy} & \varepsilon_{zz} \end{bmatrix} \tag{2}$$

and ϕ is the electric potential.

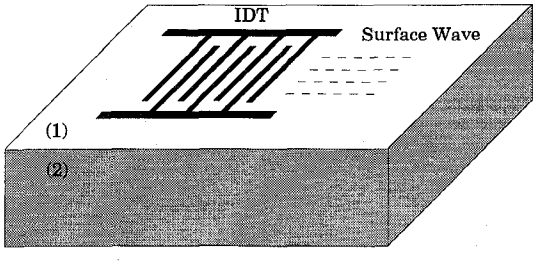

Fig. 1. Geometry of the SAW IDT.

FDM: In order to determine the potential using finite difference techniques, the entire structure is discretized in the *x*-, *y*-, and *z*-directions using non-uniform grids. The differential equation is replaced by difference equations at each point in 3-D space, which can be solved by using the overrelaxation technique. The details of this method for isotropic regions can be found in [8]. The use of this approach leads to a network interpretation [9] for the finite difference approximation to (1) at any lattice point.

For anisotropic regions this interpretation can be summarized as given below

TH 3F

CH3577-4/95/0000-1371$01.00 © 1995 IEEE

$$\phi_{i,j}^{p+1} = (1-\Omega)\,\phi_{i,j}^{p} + \frac{\Omega}{Y_{i,j}} \times \left\{ \begin{array}{l} (\phi_{i+1,j}^{p}\, Y_{i+1} + \phi_{i-1,j}^{p+1}\, Y_{i-1}) \\ +(\phi_{i,j+1}^{p}\, Y_{j+1} + \phi_{i,j-1}^{p+1}\, Y_{j-1}) \\ +(\phi_{i+1,j+1}^{p}\, Y_{i+1,j+1} + \phi_{i-1,j-1}^{p+1}\, Y_{i-1,j-1}) \\ -(\phi_{i-1,j+1}^{p}\, Y_{i-1,j+1} + \phi_{i+1,j-1}^{p+1}\, Y_{i+1,j-1}) \end{array} \right\}$$

$$Y_{i\pm1} = \left(\begin{array}{l} (\varepsilon_{i,j-1}^{yy} + \varepsilon_{i,j}^{yy}) \\ (\varepsilon_{i-1,j-1}^{yy} + \varepsilon_{i-1,j}^{yy}) \end{array} \right) \left(\frac{1}{h_i} + \frac{2}{h_i + h_{i-1}} \right) + \left(\frac{2}{h_i + h_{i-1}} \right) \left(\frac{2}{h_j + h_{j-1}} \right) \left(\varepsilon_{i,j}^{zy} + \varepsilon_{i-1,j}^{zy} - \varepsilon_{i-1,j-1}^{zy} - \varepsilon_{i,j-1}^{zy} \right) \tag{3b}$$

$$Y_{j\pm1} = \left(\begin{array}{l} (\varepsilon_{i-1,j}^{zz} + \varepsilon_{i,j}^{zz}) \\ (\varepsilon_{i-1,j-1}^{zz} + \varepsilon_{i,j-1}^{zz}) \end{array} \right) \left(\frac{1}{h_j} + \frac{2}{h_j + h_{j-1}} \right) + \left(\frac{2}{h_i + h_{i-1}} \right) \left(\frac{2}{h_j + h_{j-1}} \right) \left(\varepsilon_{i,j-1}^{yz} + \varepsilon_{i,j}^{yz} - \varepsilon_{i-1,j-1}^{yz} - \varepsilon_{i-1,j}^{yz} \right) \tag{3c}$$

$$Y_{i\pm1,j\pm1} = \left(\frac{2}{h_i + h_{i-1}} \right) \left(\frac{2}{h_j + h_{j-1}} \right) \left\{ \begin{array}{l} \varepsilon_{i,j}^{yz} + \varepsilon_{i-1,j}^{yz} + \\ \varepsilon_{i-1,j-1}^{yz} + \varepsilon_{i,j-1}^{yz} + \\ \varepsilon_{i,j}^{zy} + \varepsilon_{i-1,j}^{zy} + \\ \varepsilon_{i-1,j-1}^{zy} + \varepsilon_{i,j-1}^{zy} \end{array} \right\} \tag{3d}$$

$$Y_{i,j} = Y_{i+1} + Y_{i-1} + Y_{j+1} + Y_{j-1} \tag{3e}$$

where $Y_{i\pm1,j\pm1} = Y_{i\pm1,j\mp1}$, Ω is the over relaxation factor ranging from 1 to 2, and $h_{i,j}$'s are the distances between adjacent points in the FDM lattice, as shown in Fig. 2.

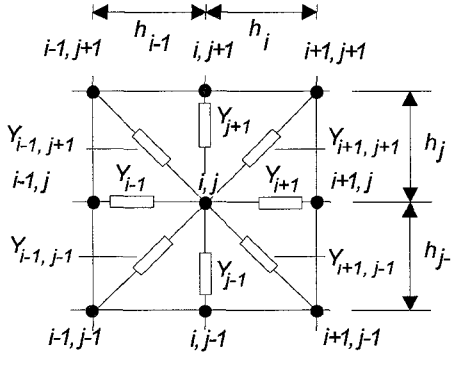

Fig. 2. Network equivalent for FD equations.

Once the potential distribution over the entire computational space is obtained, the charge on each conductor can be computed from Gauss' law:

$$Q = -\varepsilon_0 \oint_s \{[\varepsilon(x,y,z)] \cdot \nabla\phi\} \cdot \hat{n}\, ds \quad , \tag{4}$$

where $\hat{n}$ is the unit normal to the surface completely enclosing the conductor.

Acoustic Admittance: The power carried away by the acoustic wave, when a signal is applied to the SAW transducer, can be modeled as a frequency dependent admittance connected to the source. Fig. 3 shows the equivalent circuit of the SAW transducer (see Fig. 1) connected to a source with a source resistance of Rs. According to [1], the acoustic admittance , $G_a(\omega)$, of the IDT can be determined from the charge distribution making use of the relations

$$Y_a(\omega) = \omega W \Gamma_s |\bar{\rho}_e(k_o)|^2 \tag{5a}$$

$$B_a(\omega) = -Y_a(\omega) * \frac{1}{\pi\omega} \tag{5b}$$

$$G_a(\omega) = Y_a(\omega) + j\, B_a(\omega) \quad , \tag{5c}$$

where Y and B are the real and imaginary parts of the acoustic admittance (radiation conductance and susceptance), respectively. ω is the angular frequency, W is the length of the fingers, Γ_s is a material parameter and $\bar{\rho}_e(k_o)$ is the Fourier transform of the charge density. The * indicates convolution, and (5b) is the Hilbert transform of (5a).

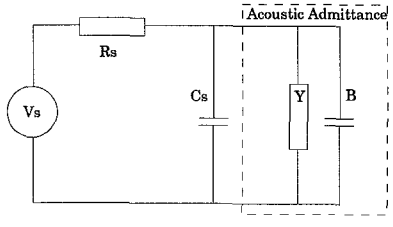

Fig. 3. Equivalent circuit of a SAW IDT; Cs is the IDT capacitance.

Once the acoustic admittance is known, equivalent circuit models can be used to analyze the SAW transducer operating in circuit conditions. In this work, the results obtained from (5a) and (5b) for a 2-D approximation are compared to those of the 3-D formulation.

The 2-D structure was simulated by taking a "cut plane" through the 3-D geometry. In order to evalute the acoustic admittance, the finger length, W, in (5a) was replaced by the overlap length of IDT fingers (see Fig. 6a). This is equivalent to neglecting the contribution of the transverse variation of charge along the fingers.

For the 3-D structure the geometry was divided into parallel tracks, as shown in Fig. 6a, and the total radiation conductance was obtained as a summation of the conductances of individual tracks:

$$Y_a(\omega) = \sum_i \omega W_i \Gamma_s |\bar{\rho}_e(k_o)|^2 \quad , \tag{5d}$$

where W_i stands for the individual track length. The corresponding radiation susceptance can then be obtained from (5b).

NUMERICAL RESULTS

In order to verify the validity of the numerical algorithm for computation of the potential inside a structure containing an anisotropic dielectric, the coupled mi-

crostrip shown in Fig. 4a was analyzed. The effects of the misaligned principal axes of the material on the impedance of the line were studied. An excellent agreement exists between previously published data [10] and results of FDM (Fig. 4b).

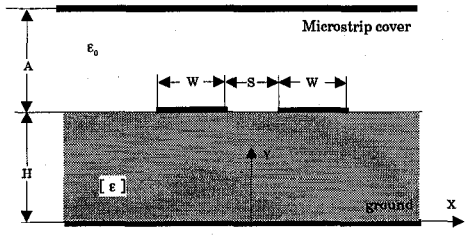

Fig. 4a. Coupled line A/H=0.5, W/H=S/H=1, ε_{xx}=40, ε_{yy}=10.

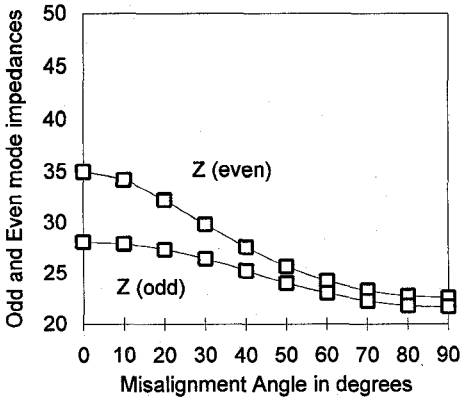

Fig. 4b. Odd/Even mode Z of coupled line (squares SDA).

To validate the calculation of the charge density, the geometry shown in Fig. 5a was examined. The calculated charge density is shown in Fig. 5b, indicating an indistinguishable agreement between the published [11] and computed data.

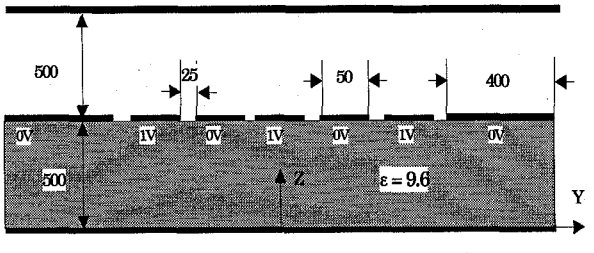

Fig. 5a. 2-D model of SAW transducer (all dimensions in μm).

To study the effects that the transverse variation of the charge density has on the acoustic admittance of the IDT, an unapodised IDT on Y-Z $LiNbO_3$ with a center frequency of 35.1 MHz was analyzed. The geometry of the IDT is shown in Figs. 6a and 6b. For the two-dimensional approximation to the problem, a cut through the three-dimensional structure was taken (Fig. 6a), and the charge density was calculated along the cutplane. To evaluate the accuracy of the acoustic admittance obtained from the 2-D formulation, the charge density was assumed to be uniform along the overlap region of the IDT fingers. In the three-dimensional simulation, the bus bars were included in the model as well. The dimensions of all structures under investigation are as shown in Figs. 6a and 6b.

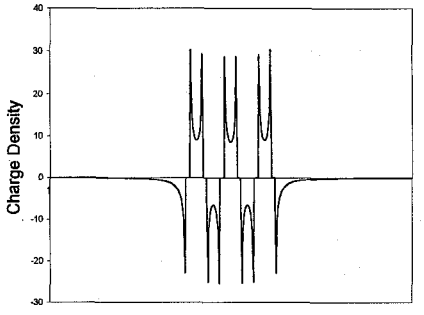

Fig. 5b. Charge density of structure in Fig. 5a. The units on the ordinate axis are 1.7708E-07 C/m^2.

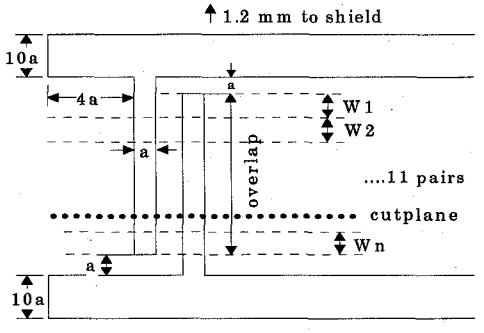

Fig. 6a. Top view of IDT fingers and bus bars.

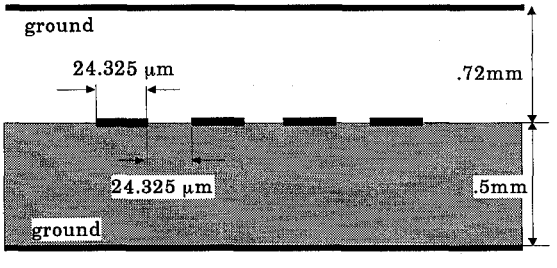

Fig. 6b. Front view of IDT. The substrate is Y-Z $LiNbO_3$.

The acoustic admittance was computed for three different lengths (60a, 10a and 5a) of electrode fingers (a is the electrode width as seen in Fig. 6a). As expected, the transverse end effects have a negligible contribution to the acoustic admittance, when the IDT finger overlap is very long (60a) (see Figs. 7a and 7b).

In most SAW applications, the apertures range from 20 - 100 λ. In structures with such dimensions, the accumulation of charge at the ends of the electrodes is mostly a perturbation to the total charge and can be neglected in calculating the acoustic admittance. This effect can also be seen in Fig. 8 for the second example, where only the radiation conductance is shown. However, as the length of the fingers becomes smaller than 10a (Fig. 8)

the error in calculating the acoustic quantities by using a two-dimensional approximation, increases. The exact differences between 2-D and 3-D results is displayed in Fig. 9 for an overlap length of 5a.

Apodised structures usually consist of regions where the overlap ranges from a very small to a large multiple of the wavelength. In such cases, the above results suggest that in the analysis of the SAW devices, when the structure needs to be discretized (MOM or FDM), a fine discretization is only needed over small overlap regions. A very coarse discretization for the longer overlap regions appears to be sufficient. From numerical standpoint, this can result in lower memory requirements and faster computation times for analysis of these structures.

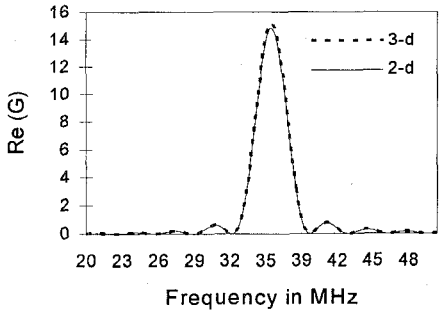

Fig. 7a. Radiation conductance in μmhos (aperture = 60a).

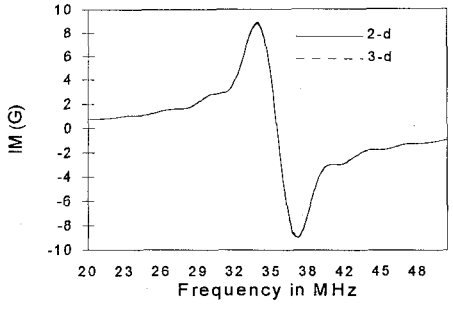

Fig. 7b. Radiation Susceptance in μmhos (aperture = 60a).

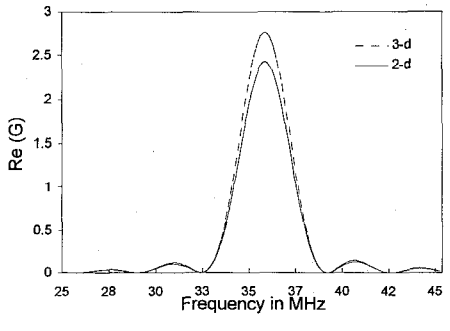

Fig. 8. Radiation conductance in μmhos (aperture = 10a).

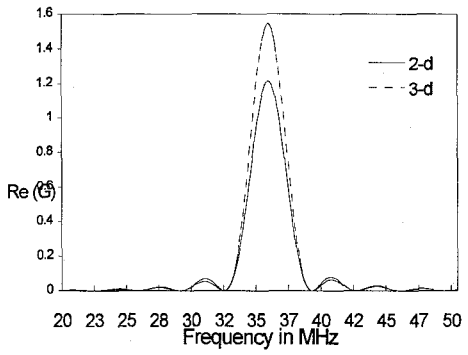

Fig. 9. Radiation conductance in μmhos (aperture = 5a).

CONCLUSION

The effects of transverse variation of charge distribution on the acoustic admittance were studied using the Finite Difference Method. The results suggest that this variation has a measurable effect only on short aperture IDTs (smaller than 10a, a is the IDT finger width). For longer lengths, this variation may be neglected. However, it is important to add, that end effect perturbations have a measurable effect on the capacitance of the IDT, which can influence its frequency response.

REFERENCES

[1] D. P. Morgan, *Surface-Wave Devices for Signal Processing*, New York: Elsevier, 1985.

[2] B. Lewis et. al, "Charge and Field Superposition methods for analysis of generalized SAW interdigital transducers," in *Proc. Ultrason. Symp.*, pp. 413-416, 1978.

[3] S. Datta, B. J. Hunsinger, and D. C. Malocha, "A Generalized Model for Periodic Transducers with Arbitrary Voltages," *IEEE Trans. Sonics Ultrasonics*, vol. SU-27, pp. 235-242, 1979.

[4] S. Datta et. al "Element factor for periodic transducers," *IEEE Trans. Sonics Ultrasonics*, vol. SU-27, pp. 42-44, 1980.

[5] R. S. Wagers, "Transverse electrostatic end effects in interdigital transducers, " in *Proc. Ultrason. Symp.*, pp. 536-539, 1976.

[6] A. R. Baghai-Wadji, S. Selberherr, and F. J. Seifert, "Rigorous 3D Electrostatic Field Analysis of SAW Transducers with Closed-Form Formulae," in *Proc. Ultrason. Symposium*, pp. 23-28, 1986.

[7] A. F. Molisch and F. J. Seifert, "Accurate Computation of the Electrostatic Charge Distribution on Shielding Plates of SAW-Transducers," *IEEE Trans. Microwave Theory Tech.*, vol. 42, no. 8, pp. 1494-1498, 1994.

[8] B. Beker and G. Cokkinides, "Computer-Aided Quasi-Static Analysis of Coplanar Transmission Lines for Microwave Integrated Circuits Using the Finite Difference Method," *Int. J. Microwave and Millimeter-Wave Computer-Aided Engineering*, vol. 4, no.1, pp. 111-119, 1994.

[9] S. R. H. Hoole, *Computer Aided Analysis and Design of Electromagnetic Devices*, Chapter 3, Elsevier, New York, 1989.

[10] M. Horno, "Quasistatic Characteristics of Covered Coupled Microstrips on Anisotropic Substrates: Spectral and Variational Analysis," *IEEE Trans. Microwave Theory Tech*, vol. 30, no. 11, pp. 1888-1892, 1982

[11] A. F. Molisch, A. R. Baghai-Wadji and C. O. Schiebl, "On the Application of the Wiener-Hopf Technique to Electrostatic Field Problems in Interdigital Transducers," *IEEE Trans. Microwave Theory Tech.*, vol. 41, no. 2, pp. 318-324, 1993.